

## Introduction

### What:

**SDG-OCC** is a lightweight yet powerful LiDAR and image fusion-based occupancy prediction method. By combining semantic and depth-guided view transformation and fusion with occupancy-driven active distillation, it achieves SOTA performance while ensuring real-time speed.

### Why:

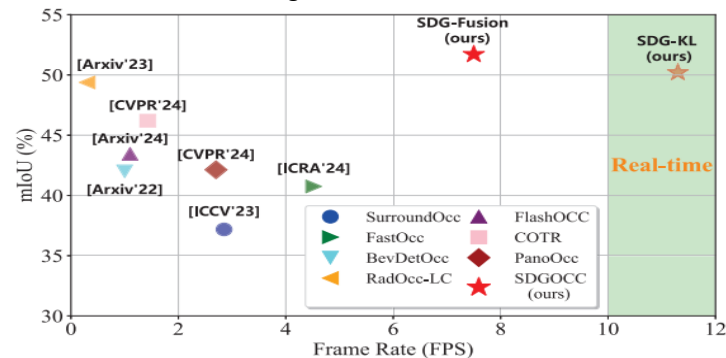
Existing methods:

- The lightweight method based on the LSS pipeline suffers from low feature utilization, leading to suboptimal performance.
- LiDAR information can enhance performance, but it introduces additional computational burden, leading to poor real-time efficiency.

### How:

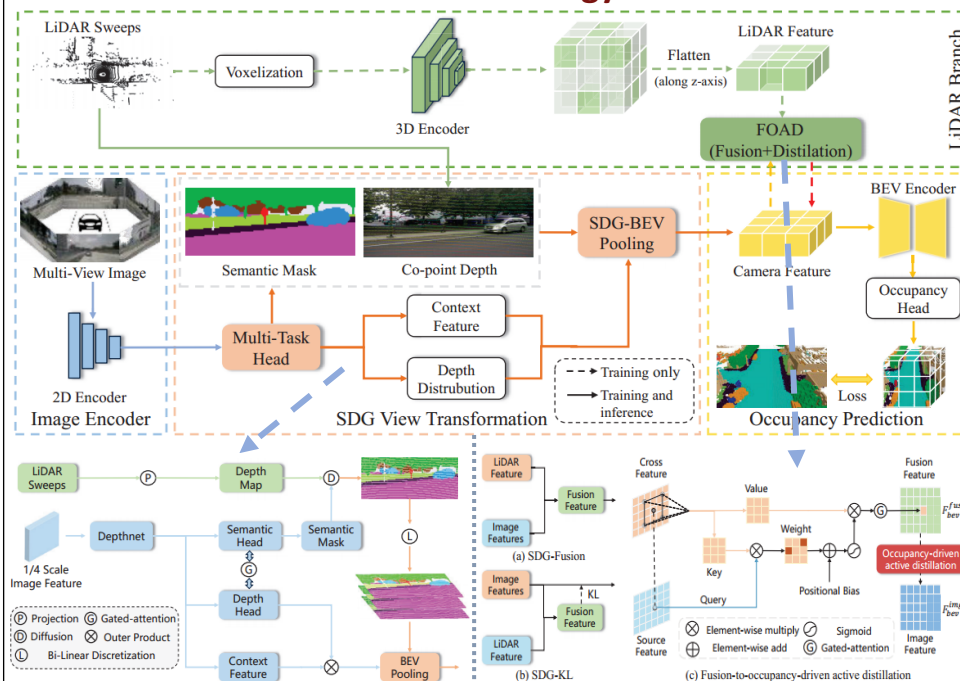
We propose:

- A view transformation method that leverages the geometric and semantic information of point clouds to guide 2D-3D transformation, significantly improving depth estimation accuracy and occupancy speed.
- An occupancy-driven active distillation module that integrates multimodal features and optimizes knowledge transfer based on LiDAR-identified regions.



Code is available at <https://github.com/DzpLab/SDGOCC>.

## Methodology

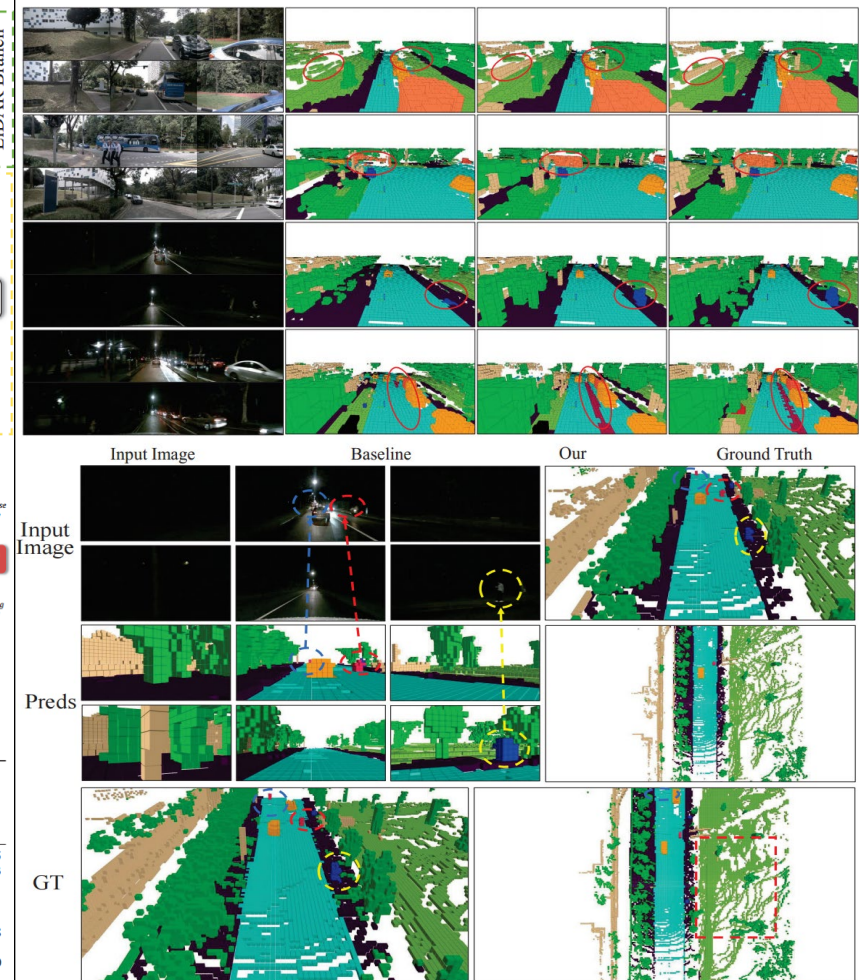


## Experiments

Effectiveness on Occ3D-nuScenes Val Dataset

| Method           | Input | Backbone | Viable Mask | mIoU  | others | barrier | bicycle | bus   | car   | const. veh. | motorcycle | pedestrian | traffic cone | trailer | truck | drive. surf. | other flat | sidewalk | terrain | manmade | vegetation | Time(ms) |
|------------------|-------|----------|-------------|-------|--------|---------|---------|-------|-------|-------------|------------|------------|--------------|---------|-------|--------------|------------|----------|---------|---------|------------|----------|
| TPVFormer [9]    | C     | R-50     | ✓           | 34.2  | 7.68   | 44.01   | 17.66   | 40.88 | 46.98 | 15.06       | 20.54      | 24.69      | 24.66        | 24.26   | 29.28 | 79.27        | 40.65      | 48.49    | 49.44   | 32.63   | 29.82      | 289.85   |
| SurroundOcc [35] | C     | R-101    | ✓           | 37.1  | 8.97   | 46.33   | 17.08   | 46.54 | 52.01 | 20.05       | 21.47      | 23.52      | 18.67        | 31.51   | 37.56 | 81.91        | 41.64      | 50.76    | 53.93   | 42.91   | 37.16      | 303.03   |
| OccFormer [44]   | C     | R-50     | ✓           | 37.4  | 9.15   | 45.84   | 18.20   | 42.80 | 50.27 | 24.00       | 20.80      | 22.86      | 20.98        | 31.94   | 38.13 | 80.13        | 38.24      | 50.83    | 54.3    | 46.41   | 40.15      | -        |
| VoxFormer [13]   | C     | R-101    | ✓           | 40.7  | -      | -       | -       | -     | -     | -           | -          | -          | -            | -       | -     | -            | -          | -        | -       | -       | -          | -        |
| FBOcc [16]       | C     | R-50     | ✓           | 42.1  | 14.30  | 49.71   | 30.0    | 46.62 | 51.54 | 29.3        | 29.13      | 29.35      | 30.48        | 34.97   | 39.36 | 83.07        | 47.16      | 55.62    | 59.88   | 44.89   | 39.58      | -        |
| PanoOcc [33]     | C     | R-101    | ✓           | 42.13 | 11.67  | 50.48   | 29.64   | 49.44 | 55.52 | 23.29       | 33.26      | 30.55      | 30.99        | 34.43   | 42.57 | 83.31        | 44.23      | 54.40    | 56.04   | 45.94   | 40.40      | 322.58   |
| FastOcc [6]      | C     | R-101    | ✓           | 40.75 | 12.86  | 46.58   | 29.93   | 46.07 | 54.09 | 23.74       | 31.10      | 30.68      | 28.52        | 33.08   | 39.69 | 83.33        | 44.65      | 53.90    | 55.46   | 42.61   | 36.50      | 221.2    |
| BEVDet4D [8]     | C     | Swin-B   | ✓           | 42.5  | 12.37  | 50.15   | 26.97   | 51.86 | 54.65 | 28.38       | 28.96      | 29.02      | 28.28        | 37.05   | 42.52 | 82.55        | 43.15      | 54.87    | 58.33   | 48.78   | 43.79      | 1000.0   |
| FlashOcc [42]    | C     | Swin-B   | ✓           | 43.52 | 13.31  | 51.62   | 28.07   | 50.91 | 55.69 | 27.46       | 31.05      | 29.98      | 29.20        | 38.86   | 43.68 | 83.87        | 45.63      | 56.33    | 59.01   | 50.63   | 44.56      | 909.1    |
| COTR [21]        | C     | Swin-B   | ✓           | 46.2  | 14.85  | 53.25   | 35.19   | 50.83 | 57.25 | 35.36       | 34.06      | 33.54      | 37.14        | 38.99   | 44.97 | 84.46        | 48.73      | 57.60    | 61.08   | 51.61   | 46.72      | 840.34   |
| HyDRa [36]       | C+L   | R-50     | ✓           | 44.40 | -      | -       | -       | -     | -     | -           | -          | -          | -            | -       | -     | -            | -          | -        | -       | -       | -          | -        |
| OCFusion [23]    | C+L   | R-101    | ✓           | 46.79 | 11.65  | 47.81   | 32.07   | 57.27 | 57.51 | 31.80       | 40.11      | 47.35      | 33.74        | 45.81   | 50.35 | 78.79        | 37.17      | 44.36    | 53.36   | 63.18   | 63.20      | -        |
| RadOcc-LC [43]   | C+L   | Swin-B   | ✓           | 49.38 | 10.93  | 58.23   | 25.01   | 57.89 | 62.85 | 34.04       | 33.45      | 50.07      | 32.05        | 48.87   | 52.11 | 82.90        | 42.73      | 55.27    | 58.34   | 68.64   | 66.01      | 3333     |
| SDG-KL           | C+L   | R-50     | ✓           | 50.16 | 12.26  | 57.12   | 23.69   | 58.77 | 62.74 | 34.55       | 36.19      | 50.1       | 32.05        | 49.89   | 51.24 | 84.1         | 46.05      | 57.2     | 61.45   | 69.56   | 65.78      | 83       |
| SDG-Fusion       | C+L   | R-50     | ✓           | 51.66 | 13.21  | 57.77   | 24.3    | 60.33 | 64.28 | 36.21       | 39.44      | 52.36      | 35.80        | 50.91   | 53.65 | 84.56        | 47.45      | 58.00    | 61.61   | 70.67   | 67.65      | 133      |

## Visualization



We anticipate that:

- The proposed SDG-OCC provides deeper insights into 2D-3D visual transformation and multimodal occupancy prediction.